NANO LETTERS

pubs.acs.org/NanoLett

Letter

Molecular Monolayer Strong Coupling in Dielectric Soft Microcavities

Adarsh B. Vasista* and William L. Barnes*

Cite This: *Nano Lett.* 2020, 20, 1766−1773

Read Online

ACCESS | Metrics & More | Article Recommendations | Supporting Information

ABSTRACT: We report strong coupling of a monolayer of J-aggregated dye molecules to the whispering gallery modes of a dielectric microsphere at room temperature. We systematically studied the evolution of strong coupling as the number of layers of dye molecules was increased and found the Rabi splitting to rise from 56 meV for a single layer to 94 meV for four layers of dye molecules. We compare our experimental results with two-dimensional (2D) numerical simulations and a simple coupled oscillator model, finding good agreement. We anticipate that these results will act as a stepping stone for integrating molecule-cavity strong coupling in a microfluidic environment since microspheres can be easily trapped and manipulated in such an environment and provide open access cavities.

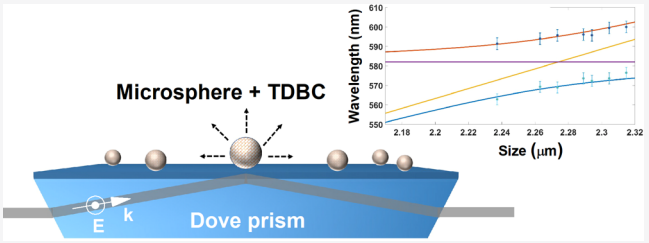

KEYWORDS: *whispering gallery modes, strong coupling, microspheres, dielectric resonators, polaritonic chemistry*

Strong coupling of molecules with cavity fields to create hybrid polariton states that have both molecular and photonic character has wide implications, not only in understanding fundamental concepts in physics[1−5] but also in a plethora of applications such as polariton-mediated energy transfer,[6,7] selective manipulation of excited states,[8] changing ground-state reactivity of a molecule,[9] polariton lasing,[10] and so forth. The strong coupling regime is attractive because in this regime the molecular energy landscape can be radically modified; the regime thus offers great opportunities to control molecular properties.[11−14] In the past, strong coupling of molecules to cavities has been explored using planar Fabry−Perot resonators,[6,15,16] single plasmonic particles,[17,18] metasurfaces,[10,19,20] and gap plasmonic cavities,[21] among others.

Because of an increasing interest in microfluidics and its many applications,[22−24] expanding the horizons of molecule-cavity coupling with mobile and controllable soft cavities, such as microspheres and vesicles, might prove useful. The obvious alternative of plasmonic nanoparticles provides subwavelength mode volumes and significant electric-field localization, making them attractive candidates to boost molecule-cavity interactions, and they also belong to a class of open cavities where molecules can be adsorbed and desorbed easily; however, plasmon modes suffer from dissipative losses and typically have broad resonance spectra. On the other hand, monolithic cavities, such as Fabry−Perot resonators, provide lower losses and narrower spectra but typically require more complex fabrication.[25] It is in this context that dielectric microspheres offer an attractive alternative. Microspheres support spectrally sharp modes called whispering gallery modes (WGMs) that have a good degree of electric-field localization.[26,27] Because of their size and composition they can be easily controlled, trapped, and moved,[28,29] and they also provide a large surface area for molecule-cavity interactions.[30,31]

Molecular strong coupling with Mie resonances in dielectric nanoparticles have been demonstrated theoretically[32,33] and experimentally.[34,35] On the other hand WGM-based cavities like microdiscs and toroids have been utilized to strongly couple atoms,[36] ions,[37] and quantum dots[38,39] at cryogenic temperatures. WGMs, in general, have been shown to exhibit exotic polarization signatures,[40] orbital angular momentum,[41] enhanced spontaneous emission,[42,43] lasing,[44] and so forth. By carefully choosing the size of the microsphere to match the resonance line width of molecular absorption, one can potentially achieve strong coupling. As strong coupling of molecules to WGMs (whispering gallery mode) of an individual microsphere has not been studied in detail, there is an imminent need to study the strong coupling of molecules to these microcavities which will expand the horizons of its applications. As a first step on this path, we study here the coupling of molecular layers of J-aggregates to polystyrene microspheres.

In this Letter, we examine the evolution of strong coupling as a function of the number of deposited layers. The signature of strong coupling was captured using single-particle dark-field scattering and the experimental results were analyzed using a coupled oscillator model, which is a well-established approach.[45]

Received: December 3, 2019
Revised: February 4, 2020
Published: February 18, 2020

https://dx.doi.org/10.1021/acs.nanolett.9b04996
Nano Lett. 2020, 20, 1766−1773

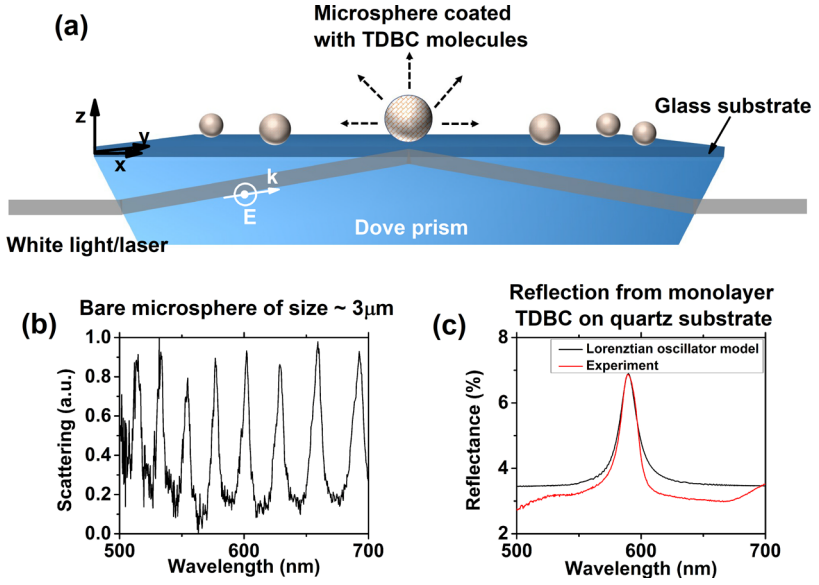

Figure 1. Schematic of experiment and spectra of "bare" cavity and "bare" molecular resonance. (a) Schematic representing the J-aggregate PDAC/TDBC coated microsphere system. Individual microspheres were probed using evanescent excitation based dark field spectroscopy. (b) Typical dark field scattering spectrum collected from a microsphere of size ~3 μm placed on glass substrate showing spectrally sharp whispering gallery modes. (c) Experimentally measured reflectance spectrum of a monolayer PDAC/TDBC on quartz substrate in comparison with that calculated using Lorenztian oscillator model.

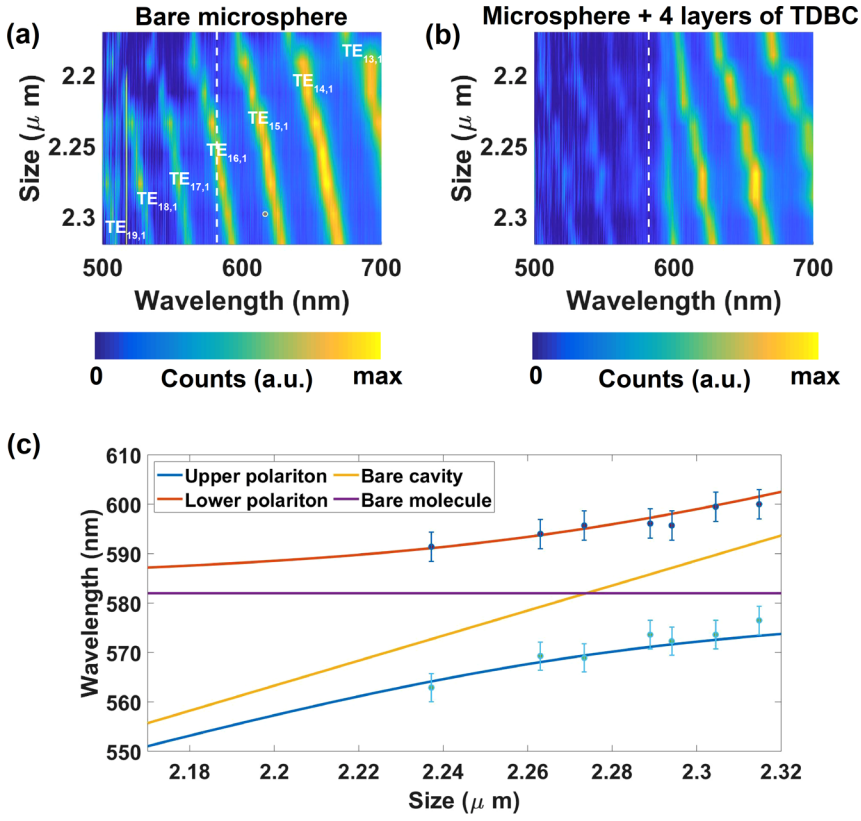

Figure 2. Strong coupling of multilayer TDBC with whispering gallery modes. (a) Experimentally measured dispersion of whispering gallery modes of a single microsphere of size ~2.23 μm. Spectra are shown as a function of microsphere size as a color map. The mode numbers of the WGMs are indicated on the dispersion plot. (b) Experimentally measured dispersion of microspheres coated with four molecular layers of TDBC showing the avoided crossing. The dashed white line represents the absorption maximum of PDAC/TDBC dye. (c) Calculated dispersion plot of the mode $TE_{16,1}$ using a coupled oscillator model to fit to the experimental data. The experimental values extracted from Figure 2b of both lower and upper polaritons are represented as dots. The experimental error in determination of the polariton peak is 1%, as indicated.

We also performed finite-element method (FEM) based numerical simulations to gain further understanding.

Figure 1a shows a schematic of the system under study. Polystyrene (PS) microspheres were coated with monomolec-

https://dx.doi.org/10.1021/acs.nanolett.9b04996
Nano Lett. 2020, 20, 1766−1773

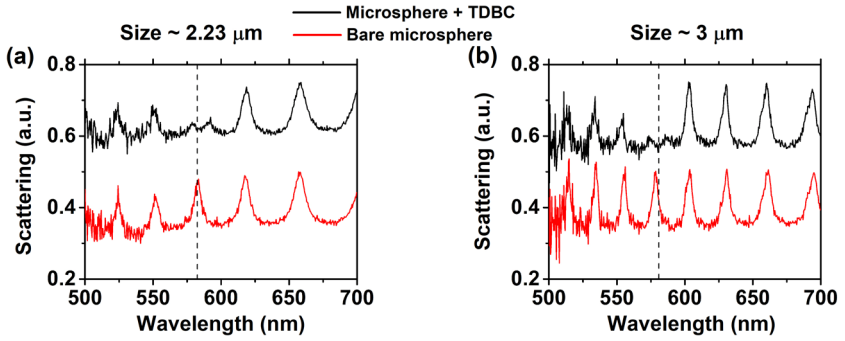

Figure 3. Dark-field spectra from individual microspheres coated with a monolayer of dye. (a) For a microsphere of size ~2.23 μm with and without deposition of a monomolecular layer of PDAC/TDBC. (b) Measured dark-field spectra from an individual microsphere of size ~3 μm with and without deposition of a monomolecular layer of PDAC/TDBC. The dashed line indicates the absorption peak of the TDBC molecules.

Table 1. Comparison of Strong Coupling Figure of Merit of Different Cavity Architectures

type of cavity	FOM ($Q/\sqrt{V}$) in $\mu m^{-3/2}$
microspheres, size ~2.23 μm (this work)	1×10^2
microspheres, size ~3 μm (this work)	2×10^2
nanotriangles[17]	6×10^3
DBR-based cavities[55,56]	$\sim 10^2$
metal clad cavities[57]	$\sim 10^2$
nanovoids[55,58]	$\sim 3 \times 10^4$

ular layers of 5,5′,6,6′-tetrachloro-1,1′-diethyl-3,3′-di(4-sulfobutyl)-benzimidazolocarbocyanine (TDBC) J-aggregate using a layer-by-layer (LBL) deposition method.[46] In our experiments, we used microspheres of two different sizes, ~3.0 and ~2.23 μm. The LBL deposition process involved alternatively depositing oppositely charged polyelectrolyte and molecular layers; further details are given in Methods.

The poly(diallyldimethylammonium chloride) (PDAC)/TDBC coated microspheres were drop-cast onto a glass coverslip and allowed to dry. Individual microspheres were then probed using a custom-built dark-field spectroscope (see

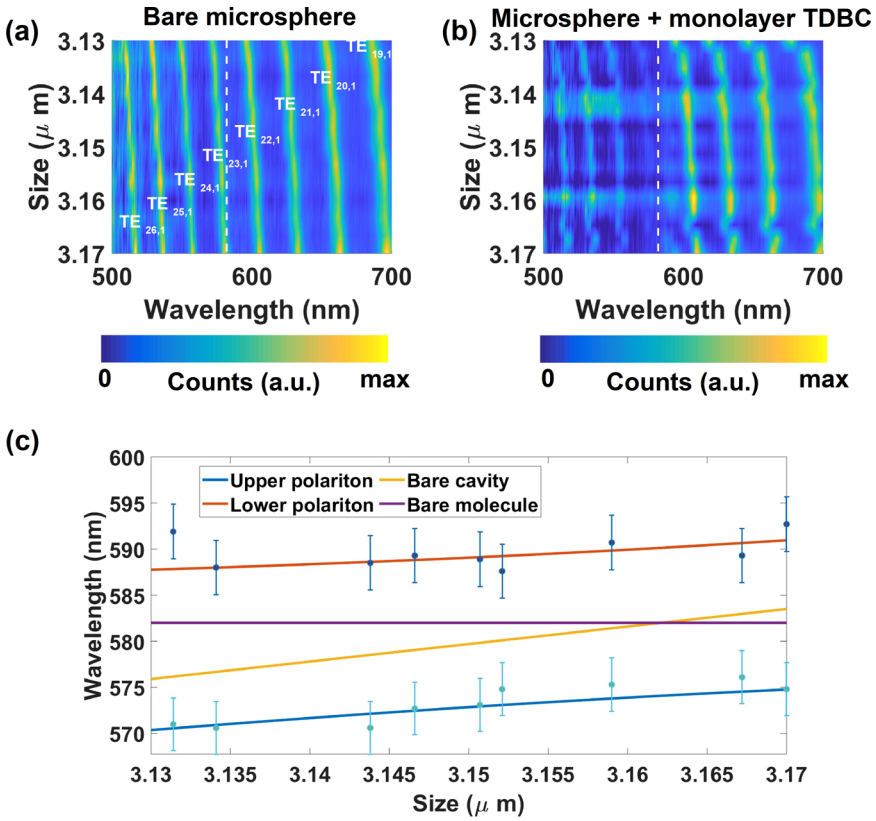

Figure 4. Strong coupling of monomolecular layer PDAC/TDBC with whispering gallery modes. (a) Experimentally measured dispersion of a whispering gallery mode of a single microsphere of size ~3 μm. (b) Experimentally measured dispersion of monomolecular layer PDAC/TDBC-coated microsphere showing avoided crossing. The dashed white line represents the absorption maximum of TDBC dye. The mode numbers of WGMs are indicated on the dispersion plot. (c) Calculated dispersion plot of the mode $TE_{23,1}$ using coupled oscillator model to fit the experimental data. The experimental values of lower and upper polaritons are represented as dots. The experimental error in determination of the polariton peak is 1%.

https://dx.doi.org/10.1021/acs.nanolett.9b04996
Nano Lett. 2020, 20, 1766−1773

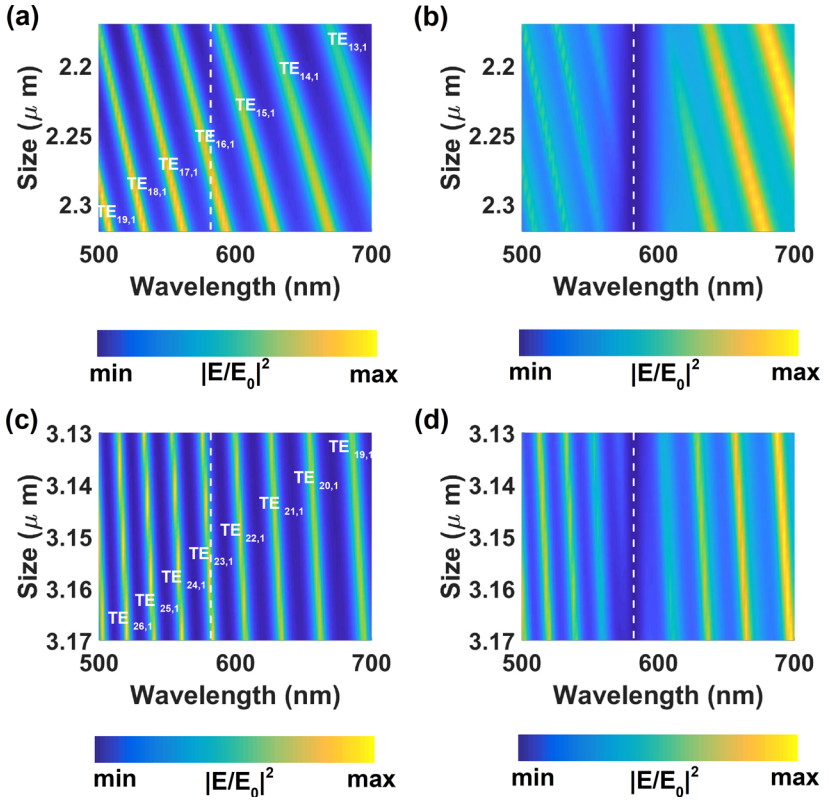

Figure 5. Simulations of strong coupling with whispering gallery modes. (a) Numerically calculated dispersion plot of whispering gallery modes of a single bare microsphere of size ∼2.23 μm. (b) Numerically calculated dispersion plot of microsphere coated with four molecular layers of PDAC/TDBC, showing avoided crossing. (c) Numerically calculated plot of whispering gallery modes of a single bare microsphere of size ∼3 μm. (d) Numerically calculated dispersion plot of microsphere coated with single molecular layer of TDBC showing avoided crossing. The dashed white line indicates the absorption maximum of PDAC/TDBC dye. The mode numbers of WGMs are indicated.

Section S1 of Supporting Information). Figure 1b shows a typical dark-field scattering spectrum of a bare microsphere of size ∼3.0 μm placed on a glass substrate for TE-polarized input. The spectral features have a line width of γ_{cavity} = 15 meV, corresponding to Q ∼ 130. Figure 1c shows the reflection spectrum of a monolayer of TDBC J-aggregate deposited on a flat quartz substrate. For comparison, we also show the calculated reflection spectrum for a monolayer TDBC J-aggregate using a transfer matrix method. Here the TDBC dye was modeled as a Lorentzian oscillator (see Section S2 of Supporting Information). The Lorentzian oscillator model reproduces the majority of optical behaviors of the LBL-deposited PDAC/TDBC system.[47]

Whispering gallery resonances have strong electric-field localization at the periphery of the microsphere so that the layer(s) of molecular J-aggregates coated on the microsphere experience an enhanced electric field. WGMs supported by microspheres can be classified as transverse electric (TE) and transverse magnetic (TM) resonances. TM modes have a radial electric-field component whereas the TE modes have a tangential field component. We chose to work with TE modes of the sphere and excite the microsphere with TE-polarized light (see Section S3 of Supporting Information). Since the microspheres were excited in evanescent configuration using a dove prism at a constant input angle keeping the wavevector of the input field constant, modes excited in the microsphere will be dependent only on the polarization of the excitation field.

We began by studying multimolecular layers rather than a single layer because the Rabi splitting ($\hbar\Omega_R$) for multimolecular systems is proportional to $\sqrt{N}$, where N is the number of molecules strongly coupled to the (cavity) field;[48] the effect of thicker layers will thus be easier to see than thin layers. We deposited four molecular layers of PDAC/TDBC on microspheres of size ∼2.23 μm. WGMs are morphology-dependent resonances and the spectral position of the resonances are critically linked to the size of the microsphere.[27] To understand and quantify strong coupling in multilayer TDBC, we plotted the dispersion of WGMs for microspheres of different sizes, but all nominally ∼2.2 μm, as shown in Figure 2a. The size of each microsphere examined was determined by adjusting the size in simulated data so as to match the spectral position of the resonances; in this way, we were also able to assign mode numbers as indicated (see Section S3 of Supporting Information). Figure 2b shows a dispersion plot of WGMs for microspheres of size ∼2.23 μm coated with four layers of PDAC/TDBC. We can see the splitting and avoided the crossing of the mode $TE_{16,1}$ near 582 nm. There is a slight blueshift in the spectral position of the avoided crossing when compared to the absorption of TDBC on a planar quartz substrate (see Section S4 of Supporting Information) and this is due to the substrate effect.[49] We also note that the reduction in scattered intensity of the modes away from the peak absorption of PDAC/TDBC molecules. This is due to the finite spectral width of molecular absorption (see Section S5 of Supporting Information for a detailed discussion on scattering losses of WGM).

The splitting of WGMs observed here is distinctively different from mode splitting due to interaction of two microspheres.

https://dx.doi.org/10.1021/acs.nanolett.9b04996
Nano Lett. 2020, 20, 1766−1773

Mode splitting in microspheres, in particular, has been studied very extensively.[50,51] This mode splitting is dependent on the distance between the microspheres and the modes excited. This near-field coupling affects all the modes sensitive to the coupling, (TE modes usually). On the other hand, microsphere−molecule coupling is sensitive to the resonance of the molecule and the spectral and spatial overlap of the molecular resonance and the microsphere resonance. In this case, mode splitting is observed only in the mode which is coupled to the molecular resonance, as seen in Figure 2b.

The polariton energies, that is, the eigenenergies of the combined hybrid system, can be determined from a coupled oscillator model as follows[6]

$$\begin{pmatrix} E_{\text{cavity}} - i\gamma_{\text{cavity}} & -g \\ -g & E_{\text{TDBC}} - i\gamma_{\text{TDBC}} \end{pmatrix} \begin{pmatrix} \alpha \\ \beta \end{pmatrix} = E_{\text{pol}} \begin{pmatrix} \alpha \\ \beta \end{pmatrix} \quad (1)$$

where E_{cavity} is the cavity resonance energy, γ_{cavity} is the cavity line width, g is the strength of coupling, E_{TDBC} is the molecular absorption energy, E_{pol} are the polariton energies of the hybrid system, and γ_{TDBC} is the line width of molecular absorption. In the present case, γ_{cavity} = 33.23 meV, γ_{TDBC} = 53 meV, and E_{TDBC} = 2.13 meV. The eigenvalues of the coupled oscillator matrix give the energies of the upper and lower polariton branches and the eigenvectors give the Hopfield coefficients.[52] Figure 2c shows the calculated dispersion curve of the mode $TE_{16,1}$ using the coupled oscillator model. By fitting this model to the experimental data, we determined that the value of g was equal to 48 meV. The Rabi splitting, given by $\hbar\Omega = \sqrt{4g^2 + \delta^2 - (\gamma_{\text{TDBC}} - \gamma_{\text{cavity}})^2}$, was then calculated to be 94 meV (for detuning $\delta = 0$). The value of $2g$ was thus more than both the molecular and the cavity resonance line widths, showing that the system studied was in the strong coupling regime. Our system thus satisfied the criterion for the occurrence of at least one complete Rabi oscillation, which translates to $g > \left[\frac{1}{4}(\gamma_{\text{cavity}} + \gamma_{\text{TDBC}}) = 21.55 \text{ meV}\right]$ and could be measured using an ultrafast time-resolved photoluminescence experiment.[53,54] The Hopfield coefficients ($|\alpha|^2$, $|\beta|^2$) measure the extent of mixing of the cavity and molecular components of the polaritonic states and are shown in Section S6 of the Supporting Information.

Having established that we could see strong coupling arising from the presence of four molecular layers of PDAC/TDBC, we next probed microspheres deposited with just a single monomolecular layer. Figure 3 shows representative spectra collected from microspheres of sizes ∼2.23 and ∼3 μm, both with and without the deposition of a monolayer of PDAC/TDBC. We see a splitting of the WGM when a monomolecular layer of PDAC/TDBC has been deposited on the sphere. The splitting of the mode is more pronounced for the ∼3 μm microsphere than for the ∼2.23 μm microsphere, something that is readily explained on the basis of larger electric-field enhancement and localization and lower radiative losses provided by microspheres of size ∼3 μm.

The extent of Rabi splitting crucially depends on the coupling parameter, g, in the system. The coupling rate, g/γ_{cavity}, can be expressed in terms of cavity quality factor (Q) and the mode volume (V) as $g/\gamma_{\text{cavity}} \propto Q\sqrt{(N/V)}$, where N is the number of molecules.[17] The value $Q/\sqrt{V}$, also called the figure of merit (FOM), affects the coupling rate and hence the Rabi splitting. The figure of merit for strong coupling calculated for a microsphere of size 3 μm is double the value of that for a microspheres of size 2.23 μm (see Table 1). Additionally, the number of molecules deposited on a microsphere of size 3 μm is more than that for a microsphere of size 2.23 μm. Hence, the coupling rate g/γ_{cavity} is larger for a microsphere of size 3 μm compared to a microsphere of size 2.23 μm. This is reflected in the Rabi splitting. We also provide the values of FOM for different architectures utilized to achieve strong coupling for comparison (see Section S7 of Supporting Information for further discussion on strong coupling figure of merit).

Hence, we chose to work with microspheres of size ∼3 μm to probe strong coupling of a monomolecular layer of PDAC/TDBC with WGMs. However, the free spectral range of WGMs for a 3 μm sphere is quite low making this size unsuitable to study multilayer coupling. The evolution of the splitting of the $TE_{16,1}$ mode for different numbers of layers of PDAC/TDBC deposited is shown in Section S8 of Supporting Information.

The experimentally measured dispersion of WGMs for microspheres of size ∼3 μm is shown in Figure 4a, together with the corresponding mode numbers. The deposition of a monolayer of PDAC/TDBC on the microsphere results in a splitting of the $TE_{23,1}$ mode, as shown in Figure 4b. To quantify the coupling, we calculated the value of the coupling strength, g, using the coupled oscillator model as described earlier. In the case of microspheres of size ∼3 μm and γ_{cavity} = 15 meV, we kept γ_{TDBC} as before. We can thus plot the dispersion of the hybridized $TE_{23,1}$ mode, shown in Figure 4c; the value of g was found to be 35 meV. The value of the coupling strength, $2g$, was larger than both cavity and molecular line widths, again showing that this system was in the strong coupling regime. The calculated value of the Rabi-splitting, $\hbar\Omega_R$, was equal to 59 meV. For comparison, the measured dark-field spectra for different detunings in the case of a monomolecular layer of TDBC coated on microspheres of size ∼2.23 μm are shown in Section S9 of Supporting Information.

To gain further understanding of the system, we performed 2D finite-element method (FEM) modeling of the hybrid system using COMSOL multiphysics.[59] The microsphere was excited using a TE-polarized broadband source in evanescent excitation configuration (see Section S10 of the Supporting Information for details on modeling). Figure 5a shows the dispersion of WGMs for individual microspheres of size ∼2.23 μm. To model the coupling between the PDAC/TDBC molecular layer and WGMs, a shell of thickness 6.8 nm (1.7 nm × 4) was introduced.[46] The resulting dispersion plot is shown in Figure 5b. The simulated dispersion plot agrees well with the experimental data, showing an avoided crossing at 582 nm. The Rabi splitting was found to be 119 meV. The mismatch between the calculated (119 meV) and experimentally (96 meV) measured values was probably due to a combination of imperfect coverage of molecules on the microsphere and an orientation mismatch of the molecular transitional dipole moment with respect to the polarization of the mode (see Section S11 of Supporting Information for a discussion on homogeneity of coverage). To further establish strong coupling between monolayer TDBC with WGMs, we also show avoided crossing in absorption spectra of the coupled system, see Section S10 of Supporting Information. We calculated the Hopfield coefficients using the coupled oscillator model with g = 60.53 meV (corresponding to $\hbar\Omega_R$ = 119 meV), shown in Section S6 of Supporting Information. We also note that the intensity of polariton modes is low in both absorption and scattering spectra.

https://dx.doi.org/10.1021/acs.nanolett.9b04996
Nano Lett. 2020, 20, 1766−1773

This is due to the coupling losses associated with the excitation of WGMs in the microsphere.

A numerically calculated dispersion plot of the WGMs supported by an individual ∼3 μm microsphere is shown in Figure 5c. To simulate the interaction between molecular layer and WGMs, we introduced a shell of thickness 1.7 nm around the microsphere. The resulting dispersion plot is shown in Figure 5d, and the mode $TE_{23,1}$ splits into two and undergoes an avoided crossing at around 582 nm, which is in agreement with the experimental results; the calculated value of Rabi splitting in this case was $\hbar\Omega_R$ = 65 meV. The calculated absorption spectra of the system lends further support to the system being in the strong coupling regime by showing a clear mode splitting and anticrossing (see Section S10 of Supporting Information). The Hopfield coefficients calculated using the coupled oscillator model, for the mode $TE_{23,1}$, are shown in Section S6 of Supporting Information.

Finally, we note that we also made preliminary experiments to look at the photoluminescence (PL) of our systems. We found that the PL spectra of our system were dependent on the mode of excitation/collection, as noted before.[60] Nonetheless, our data show that some of the PL arises from the lower polariton mode; details are presented in Section S12 of Supporting Information.

In summary, we have shown strong coupling between a single dye monolayer and the whispering gallery modes of a soft dielectric cavity. We studied the evolution of the strong coupling as the number of monolayers of our dye system, PDAC/TDBC, was increased, finding that the splitting increased, as expected. We supported our experimental results with numerically simulated data. This study provides a new launch point for polaritonic chemistry by providing a new open cavity system that is ideally suited to microfluidic systems and applications. Furthermore, the microsphere dielectric cavities we have employed should be well suited to optical trapping and thus manipulation. The results presented here may also be extended to study strong coupling between transition metal dichalcogenides and microsphere supporting modes with angular momentum.

METHODS

For the layer-by-layer fabrication, we used a cationic PDAC solution as the polyelectrolyte binder for anionic TDBC J-aggregate solution. A typical deposition step consists of mixing 20 μL of PDAC solution (20% by weight in water, diluted 1:1000) with 1 mL of PS microsphere colloidal solution (15% by weight in water, diluted 50 times) and allowing to settle for 20 min. The solution was then washed three times in water to remove excess polyelectrolyte solution. This step forms a positively charged layer of PDAC on microspheres. Then 100 μL of TDBC solution (0.01 M) was added to the microsphere/PDAC colloid and kept for 20 min. The solution was then washed three times in water to remove excess TDBC molecules. This procedure was repeated to deposit multiple layers of J-aggregate TDBC on the microsphere surface. Finally the TDBC layer was protected by depositing a layer of PDAC molecules.

ASSOCIATED CONTENT

Supporting Information

The Supporting Information is available free of charge at https://pubs.acs.org/doi/10.1021/acs.nanolett.9b04996.

Simulation strategy and dark-field scattering spectra from microspheres (PDF)

AUTHOR INFORMATION

Corresponding Authors

Adarsh B. Vasista − *Department of Physics and Astronomy, University of Exeter, Exeter EX44QL, United Kingdom;* orcid.org/0000-0001-7641-8647; Email: a.vasista@exeter.ac.uk

William L. Barnes − *Department of Physics and Astronomy, University of Exeter, Exeter EX44QL, United Kingdom;* orcid.org/0000-0002-9474-5534; Email: w.l.barnes@exeter.ac.uk

Complete contact information is available at: https://pubs.acs.org/10.1021/acs.nanolett.9b04996

Notes

The authors declare no competing financial interest.

ACKNOWLEDGMENTS

A.B.V. would like to thank Wai Jue Tan for his help in preparing samples. The authors acknowledge the support of European Research Council through the Photmat project (ERC-2016-AdG-742222 www.photmat.eu). A.B.V. acknowledges fruitful discussions with Rohit Chikkaraddy during the initial stages of the work.

REFERENCES

(1) Leroux, C.; Govia, L. C. G.; Clerk, A. A. Enhancing Cavity Quantum Electrodynamics via Antisqueezing: Synthetic Ultrastrong Coupling. *Phys. Rev. Lett.* **2018**, *120*, 093602.

(2) Flick, J.; Ruggenthaler, M.; Appel, H.; Rubio, A. Atoms and molecules in cavities, from weak to strong coupling in quantum-electrodynamics (QED) chemistry. *Proc. Natl. Acad. Sci. U. S. A.* **2017**, *114*, 3026−3034.

(3) Canaguier-Durand, A.; Devaux, E.; George, J.; Pang, Y.; Hutchison, J. A.; Schwartz, T.; Genet, C.; Wilhelms, N.; Lehn, J.-M.; Ebbesen, T. W. Thermodynamics of Molecules Strongly Coupled to the Vacuum Field. *Angew. Chem., Int. Ed.* **2013**, *52*, 10533−10536.

(4) Vasista, A. B.; Jog, H.; Heilpern, T.; Sykes, M. E.; Tiwari, S.; Sharma, D. K.; Chaubey, S. K.; Wiederrecht, G. P.; Gray, S. K.; Kumar, G. V. P. Differential Wavevector Distribution of Surface-Enhanced Raman Scattering and Fluorescence in a Film-Coupled Plasmonic Nanowire Cavity. *Nano Lett.* **2018**, *18*, 650−655.

(5) Ojambati, O. S.; Chikkaraddy, R.; Deacon, W. D.; Horton, M.; Kos, D.; Turek, V. A.; Keyser, U. F.; Baumberg, J. J. Quantum electrodynamics at room temperature coupling a single vibrating molecule with a plasmonic nanocavity. *Nat. Commun.* **2019**, *10*, 1−7.

(6) Coles, D. M.; Somaschi, N.; Michetti, P.; Clark, C.; Lagoudakis, P. G.; Savvidis, P. G.; Lidzey, D. G. Polariton-mediated energy transfer between organic dyes in a strongly coupled optical microcavity. *Nat. Mater.* **2014**, *13*, 712−719.

(7) Zhong, X.; Chervy, T.; Zhang, L.; Thomas, A.; George, J.; Genet, C.; Hutchison, J. A.; Ebbesen, T. W. Energy Transfer between Spatially Separated Entangled Molecules. *Angew. Chem., Int. Ed.* **2017**, *56*, 9034−9038.

(8) Stranius, K.; Hertzog, M.; Börjesson, K. Selective manipulation of electronically excited states through strong light−matter interactions. *Nat. Commun.* **2018**, *9*, 1−7.

(9) Thomas, A.; Lethuillier-Karl, L.; Nagarajan, K.; Vergauwe, R. M. A.; George, J.; Chervy, T.; Shalabney, A.; Devaux, E.; Genet, C.; Moran, J.; Ebbesen, T. W. Tilting a ground-state reactivity landscape by vibrational strong coupling. *Science* **2019**, *363*, 615−619.

(10) Ramezani, M.; Halpin, A.; Fernández-Domínguez, A. I.; Feist, J.; Rodriguez, S. R.-K.; Garcia-Vidal, F. J.; Rivas, J. G. Plasmon-exciton-polariton lasing. *Optica* **2017**, *4*, 31−37.
(11) Hertzog, M.; Wang, M.; Mony, J.; Börjesson, K. Strong light−matter interactions: a new direction within chemistry. *Chem. Soc. Rev.* **2019**, *48*, 937−961.
(12) Schäfer, C.; Ruggenthaler, M.; Appel, H.; Rubio, A. Modification of excitation and charge transfer in cavity quantum-electrodynamical chemistry. *Proc. Natl. Acad. Sci. U. S. A.* **2019**, *116*, 4883−4892.
(13) Ribeiro, R. F.; Martínez-Martínez, L. A.; Du, M.; Campos-Gonzalez-Angulo, J.; Yuen-Zhou, J. Polariton chemistry: controlling molecular dynamics with optical cavities. *Chemical Science* **2018**, *9*, 6325−6339.
(14) Ebbesen, T. W. Hybrid Light−Matter States in a Molecular and Material Science Perspective. *Acc. Chem. Res.* **2016**, *49*, 2403−2412.
(15) Lidzey, D. G.; Bradley, D. D. C.; Virgili, T.; Armitage, A.; Skolnick, M. S.; Walker, S. Room Temperature Polariton Emission from Strongly Coupled Organic Semiconductor Microcavities. *Phys. Rev. Lett.* **1999**, *82*, 3316−3319.
(16) Shalabney, A.; George, J.; Hutchison, J.; Pupillo, G.; Genet, C.; Ebbesen, T. W. Coherent coupling of molecular resonators with a microcavity mode. *Nat. Commun.* **2015**, *6*, 1−6.
(17) Zengin, G.; Wersäll, M.; Nilsson, S.; Antosiewicz, T. J.; Käll, M.; Shegai, T. Realizing Strong Light-Matter Interactions between Single-Nanoparticle Plasmons and Molecular Excitons at Ambient Conditions. *Phys. Rev. Lett.* **2015**, *114*, 157401.
(18) Wersäll, M.; Cuadra, J.; Antosiewicz, T. J.; Balci, S.; Shegai, T. Observation of Mode Splitting in Photoluminescence of Individual Plasmonic Nanoparticles Strongly Coupled to Molecular Excitons. *Nano Lett.* **2017**, *17*, 551−558.
(19) Dintinger, J.; Klein, S.; Bustos, F.; Barnes, W. L.; Ebbesen, T. W. Strong coupling between surface plasmon-polaritons and organic molecules in subwavelength hole arrays. *Phys. Rev. B: Condens. Matter Mater. Phys.* **2005**, *71*, 035424.
(20) Ramezani, M.; Berghuis, M.; Rivas, J. G. Strong light−matter coupling and exciton-polariton condensation in lattices of plasmonic nanoparticles. *J. Opt. Soc. Am. B* **2019**, *36*, E88−E103.
(21) Chikkaraddy, R.; de Nijs, B.; Benz, F.; Barrow, S. J.; Scherman, O. A.; Rosta, E.; Demetriadou, A.; Fox, P.; Hess, O.; Baumberg, J. J. Single-molecule strong coupling at room temperature in plasmonic nanocavities. *Nature* **2016**, *535*, 127−130.
(22) MacDonald, M. P.; Spalding, G. C.; Dholakia, K. Microfluidic sorting in an optical lattice. *Nature* **2003**, *426*, 421−424.
(23) Paterson, L.; MacDonald, M. P.; Arlt, J.; Sibbett, W.; Bryant, P. E.; Dholakia, K. Controlled Rotation of Optically Trapped Microscopic Particles. *Science* **2001**, *292*, 912−914.
(24) Ashkin, A.; Dziedzic, J. Optical trapping and manipulation of viruses and bacteria. *Science* **1987**, *235*, 1517−1520.
(25) Bahsoun, H.; Chervy, T.; Thomas, A.; Börjesson, K.; Hertzog, M.; George, J.; Devaux, E.; Genet, C.; Hutchison, J. A.; Ebbesen, T. W. Electronic Light−Matter Strong Coupling in Nanofluidic Fabry−Pérot Cavities. *ACS Photonics* **2018**, *5*, 225−232.
(26) Vahala, K. J. Optical microcavities. *Nature* **2003**, *424*, 839−846.
(27) Bohren, C. F.; Huffman, D. R. *Absorption and Scattering of Light by Small Particles*; Wiley Online Library, 1998.
(28) Ashkin, A.; Dziedzic, J. M.; Bjorkholm, J. E.; Chu, S. Observation of a single-beam gradient force optical trap for dielectric particles. *Opt. Lett.* **1986**, *11*, 288−290.
(29) Ashkin, A. Optical trapping and manipulation of neutral particles using lasers. *Proc. Natl. Acad. Sci. U. S. A.* **1997**, *94*, 4853−4860.
(30) Ashkin, A.; Dziedzic, J. M.; Bjorkholm, J. E.; Chu, S. Observation of a single-beam gradient force optical trap for dielectric particles. *Opt. Lett.* **1986**, *11*, 288−290.
(31) Neuman, K. C.; Block, S. M. Optical trapping. *Rev. Sci. Instrum.* **2004**, *75*, 2787−2809.
(32) Tserkezis, C.; Gonçalves, P. A. D.; Wolff, C.; Todisco, F.; Busch, K.; Mortensen, N. A. Mie excitons: Understanding strong coupling in dielectric nanoparticles. *Phys. Rev. B: Condens. Matter Mater. Phys.* **2018**, *98*, 155439.
(33) Gentile, M. J.; Barnes, W. L. Hybridised exciton−polariton resonances in core−shell nanoparticles. *J. Opt.* **2017**, *19*, 035003.
(34) Wang, H.; Ke, Y.; Xu, N.; Zhan, R.; Zheng, Z.; Wen, J.; Yan, J.; Liu, P.; Chen, J.; She, J.; Zhang, Y.; Liu, F.; Chen, H.; Deng, S. Resonance Coupling in Silicon Nanosphere−J-Aggregate Heterostructures. *Nano Lett.* **2016**, *16*, 6886−6895.
(35) Ruan, Q.; Li, N.; Yin, H.; Cui, X.; Wang, J.; Lin, H.-Q. Coupling between the Mie Resonances of Cu2O Nanospheres and the Excitons of Dye Aggregates. *ACS Photonics* **2018**, *5*, 3838−3848.
(36) Aoki, T.; Dayan, B.; Wilcut, E.; Bowen, W. P.; Parkins, A. S.; Kippenberg, T. J.; Vahala, K. J.; Kimble, H. J. Observation of strong coupling between one atom and a monolithic microresonator. *Nature* **2006**, *443*, 671−674.
(37) Farr, W. G.; Goryachev, M.; Creedon, D. L.; Tobar, M. E. Strong coupling between whispering gallery modes and chromium ions in ruby. *Phys. Rev. B: Condens. Matter Mater. Phys.* **2014**, *90*, 054409.
(38) Srinivasan, K.; Painter, O. Linear and nonlinear optical spectroscopy of a strongly coupled microdisk−quantum dot system. *Nature* **2007**, *450*, 862−865.
(39) Peter, E.; Senellart, P.; Martrou, D.; Lemaître, A.; Hours, J.; Gérard, J. M.; Bloch, J. Exciton-Photon Strong-Coupling Regime for a Single Quantum Dot Embedded in a Microcavity. *Phys. Rev. Lett.* **2005**, *95*, 067401.
(40) Vasista, A. B.; Tiwari, S.; Sharma, D. K.; Chaubey, S. K.; Kumar, G. V. P. Vectorial Fluorescence Emission from Microsphere Coupled to Gold Mirror. *Adv. Opt. Mater.* **2018**, *6*, 1801025.
(41) Cai, X.; Wang, J.; Strain, M. J.; Johnson-Morris, B.; Zhu, J.; Sorel, M.; O'Brien, J. L.; Thompson, M. G.; Yu, S. Integrated Compact Optical Vortex Beam Emitters. *Science* **2012**, *338*, 363−366.
(42) Melnikau, D.; Savateeva, D.; Chuvilin, A.; Hillenbrand, R.; Rakovich, Y. P. Whispering gallery mode resonators with J-aggregates. *Opt. Express* **2011**, *19*, 22280−22291.
(43) Melnikau, D.; Savateeva, D.; Rusakov, K. I.; Rakovich, Y. P. Whispering gallery mode emission from a composite system of J-aggregates and photonic microcavity. *J. Lumin.* **2014**, *145*, 138−143.
(44) Feng, L.; Wong, Z. J.; Ma, R.-M.; Wang, Y.; Zhang, X. Single-mode laser by parity-time symmetry breaking. *Science* **2014**, *346*, 972−975.
(45) Wersäll, M.; Munkhbat, B.; Baranov, D. G.; Herrera, F.; Cao, J.; Antosiewicz, T. J.; Shegai, T. Correlative Dark-Field and Photoluminescence Spectroscopy of Individual Plasmon−Molecule Hybrid Nanostructures in a Strong Coupling Regime. *ACS Photonics* **2019**, *6*, 2570−2576.
(46) Bradley, M. S.; Tischler, J. R.; Bulović, V. Layer-by-Layer J-Aggregate Thin Films with a Peak Absorption Constant of 106 cm^{-1}. *Adv. Mater.* **2005**, *17*, 1881−1886.
(47) Gentile, M. J.; Núñez-Sánchez, S.; Barnes, W. L. Optical Field-Enhancement and Subwavelength Field-Confinement Using Excitonic Nanostructures. *Nano Lett.* **2014**, *14*, 2339−2344.
(48) Törmä, P.; Barnes, W. L. Strong coupling between surface plasmon polaritons and emitters: a review. *Rep. Prog. Phys.* **2015**, *78*, 013901.
(49) Nabetani, A.; Tomioka, A.; Tamaru, H.; Miyano, K. Optical properties of two-dimensional dye aggregate. *J. Chem. Phys.* **1995**, *102*, 5109−5117.
(50) Smith, D. D.; Chang, H.; Fuller, K. A. Whispering-gallery mode splitting in coupled microresonators. *J. Opt. Soc. Am. B* **2003**, *20*, 1967−1974.
(51) Fuller, K. A. Some novel features of morphology dependent resonances of bispheres. *Appl. Opt.* **1989**, *28*, 3788−3790.
(52) Hopfield, J. J. Theory of the Contribution of Excitons to the Complex Dielectric Constant of Crystals. *Phys. Rev.* **1958**, *112*, 1555−1567.
(53) Khitrova, G.; Gibbs, H. M.; Kira, M.; Koch, S. W.; Scherer, A. Vacuum Rabi splitting in semiconductors. *Nat. Phys.* **2006**, *2*, 81−90.
(54) Pelton, M.; Storm, S. D.; Leng, H. Strong coupling of emitters to single plasmonic nanoparticles: exciton-induced transparency and Rabi splitting. *Nanoscale* **2019**, *11*, 14540−14552.

https://dx.doi.org/10.1021/acs.nanolett.9b04996
Nano Lett. 2020, 20, 1766−1773

(55) Dovzhenko, D. S.; Ryabchuk, S. V.; Rakovich, Yu. P.; Nabiev, I. R. Light−matter interaction in the strong coupling regime: configurations, conditions, and applications. *Nanoscale* **2018**, *10*, 3589−3605.
(56) Liu, X.; Galfsky, T.; Sun, Z.; Xia, F.; Lin, E.-c.; Lee, Y.-H.; Kéna-Cohen, S.; Menon, V. M. Strong light−matter coupling in two-dimensional atomic crystals. *Nat. Photonics* **2015**, *9*, 30−34.
(57) Kai, K.; Oh-Hara, C.; Inoue, H.; Yamanaka, T.; Ujihara, K. Measurement of the Characteristic Transverse Mode Radius of a Planar Microcavity Laser. *Jpn. J. Appl. Phys.* **2002**, *41*, 7398−7399.
(58) Sugawara, Y.; Kelf, T. A.; Baumberg, J. J.; Abdelsalam, M. E.; Bartlett, P. N. Strong Coupling between Localized Plasmons and Organic Excitons in Metal Nanovoids. *Phys. Rev. Lett.* **2006**, *97*, 266808.
(59) *COMSOL: Multiphysics Software*; 2019.
(60) Baieva, S.; Ihalainen, J. A.; Toppari, J. J. Strong coupling between surface plasmon polaritons and β-carotene in nanolayered system. *J. Chem. Phys.* **2013**, *138*, 044707.

https://dx.doi.org/10.1021/acs.nanolett.9b04996
Nano Lett. 2020, 20, 1766−1773